

# DC, LOW FREQUENCY AND RF DRIFT IN AlGaAs/InGaAs PM-HEMTs BIASED IN HIGH FIELD AND HIGH POWER DISSIPATION REGIME

G. Meneghesso<sup>(1)</sup>, A. Paccagnella<sup>(1)</sup>, G. Martines<sup>(2)</sup>, F. Garat<sup>(3)</sup>, C. Crosato<sup>(1)</sup>,  
E. Zanoni<sup>(1)</sup>

1) Università di Padova, Dipartimento di Elettronica ed Informatica,  
via Gradenigo 6/A, 35131 Padova, Italy, IMFM Padova and Consorzio Padova Ricerche.  
tel. +39-049-8277664, fax. +39-049-8277699, e-mail: gauss@dei.unipd.it.

2) Università di Cagliari, Dip. di Ing. Elettrica ed Elettronica,  
Piazza d, Armi, 09123 Cagliari, Italy

3) European Space Agency ESTEC, Kaplerlaan 1, P.O.BOX 299,  
AG Noordwijk ZH, The Netherlands.

## ABSTRACT

*In this work we analyze degradation phenomena observed in pseudomorphic AlGaAs/InGaAs HEMTs with Al/Ti gate metallization, which have been submitted to accelerated tests at high drain-source voltage  $V_{DS}$  and high power dissipation  $P_D$ . After these tests, we observe permanent degradation effects, consisting in electron trapping in the gate-drain access region, with consequent decrease in the longitudinal electric field and 'breakdown walkout', and in thermally-activated interdiffusion of the Al/Ti gate with decrease in the gate Schottky barrier height and increase in drain saturation current  $I_D$ . Rather than causing a degradation of the rf characteristics of the device, these phenomena induce an increase in the associated rf gain at 12 GHz, the other rf characteristics being almost unchanged. Overall, the most relevant failure mode observed is an increase of low-frequency transconductance.*

## INTRODUCTION

The long term stability in AlGaAs/-InGaAs/GaAs pseudomorphic HEMT's (PM-HEMT's) is of crucial importance for their application in the high frequency and low noise application such as satellites and radar. Recoverable degradation has already been observed in commercially available AlGaAs/InGaAs PM-HEMT's [1], [2]. Interaction between impact-ionization phenomena and traps has been pointed out as the responsible for the observed instabilities.

The recoverable drift observed derived from the trapping/de-trapping of hot-electrons, and/or from the recombination of holes generated by impact-ionization with electron trapped in deep levels. Permanent hot-electron induced degradation has been observed in conventional commercially available AlGaAs/GaAs HEMTs [3] and in prototype AlGaAs/InGaAs PM-HEMTs [4]. On the other hand, several failure mechanisms induced by thermally-activated metal-semiconductor interdiffusion have been reported by G. Meneghesso et al. in [5].

In this work we analyze degradation phenomena observed in pseudomorphic AlGaAs/InGaAs HEMTs with Al/Ti gate metallization, which have been submitted to accelerated tests at high drain-source voltage  $V_{DS}$  and high power dissipation  $P_D$ . Main results can be summarized as follows:



- (a) Untreated devices are already affected by trapping effects: traps having an activation energy  $E_a=0.4$  eV are located in the gate-drain and gate-source access regions; other traps with  $E_a=0.35$  eV can be found in the AlGaAs donor layer under the gate and may be identified as DX centers.
- (b) The simultaneous presence of these traps and of the impact-ionization phenomena induces a noticeable kink in the output I-V curves [6].

After hot electron and high power dissipation tests, we observe permanent degradation effects, consisting in:

- (c) Electron trap generation in the gate-drain access region, with consequent decrease in the longitudinal electric field and "breakdown walkout" [4];
- (d) Thermally-activated interdiffusion of the Al/Ti gate with decrease in the gate Schottky barrier height and increase in drain saturation current  $I_D$ . Rather than causing a degradation of the rf characteristics of the device, these phenomena induce an increase in the associated rf gain at 12 GHz, the other rf characteristics being almost unchanged. Overall, the most relevant failure mode observed is an increase of low-frequency transconductance, especially at low temperature.

### DEVICES AND EXPERIMENTAL TESTS

Tested devices were commercially-available  $0.25 \mu\text{m}$  Al/Ti gate pseudomorphic HEMTs having a gate width  $W = 200 \mu\text{m}$ ; the AlGaAs donor layer was Si-doped; the gate has a mushroom shape in order to reduce the gate resistance and parasitic capacitance and improve the power handling capability. A complete DC, rf and low frequency characterization has been carried out on untreated devices and at regular times during accelerated tests. Devices have been stressed in different bias points corresponding to different power dissipations and channel temperatures and to different values of the maximum electric field in the gate-drain access region, the lowest stress level being  $V_{DS} = 4$  V and  $V_{GS} = 0$  V, with minimum power dissipation  $P_D = 270$  mW and channel temperature  $T_{CH} = 230$  °C, hereafter identified as stress "A"; other two tests "B" and "C": "B" has  $V_{DS} = 5.5$  V and  $V_{GS} = 0$  V, with  $P_D = 440$  mW and  $T_{ch} = 355$ °C. This test has the highest power dissipation and channel temperature. "C" was carried out at  $V_{DS} = 5.5$  V and  $V_{GS} = -0.2$  V, with  $P_D = 360$  mW and channel temperature  $T_{ch} = 300$  °C.

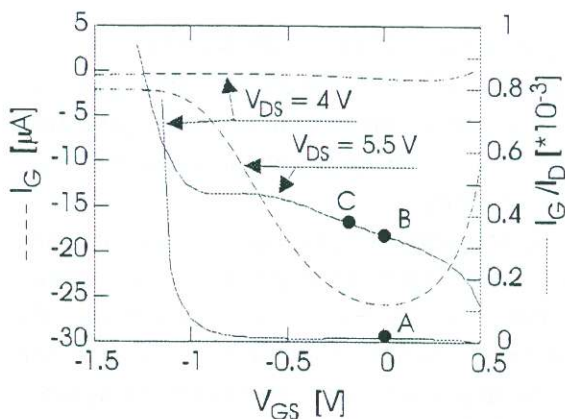


**Fig.1.**  $I_G$  (dashed lines) and  $I_G/I_D$  (continuous lines) measured at  $V_{DS}=4$  V and 5.5V. The different bias points, adopted for accelerated testing, are indicated.

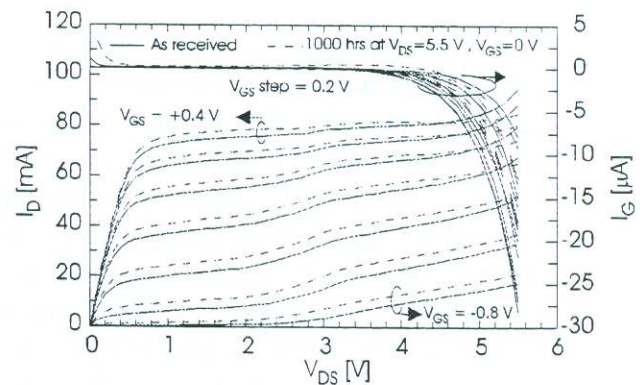


**Fig. 2.**  $I_D$  and  $I_G$  vs  $V_{DS}$  at different  $V_{GS}$  before (continuous lines) and after (dashed lines) accelerated life tests in the "B" bias point.



Figure 1 shows the gate current,  $I_G$ , and the gate current-to-drain current ratio,  $I_G/I_D$ , vs the gate to source voltage,  $V_{GS}$ , measured in an untreated device at  $V_{DS} = 4$  V and 5.5 V. The typical bell shape behavior of the  $I_G$  (due to collection of holes generated by impact-ionization) is almost not visible at low  $V_{DS}$  ( $V_{DS} = 4$  V) following the reduction of the electric field. The  $I_G/I_D$  ratio, proportional to the multiplication factor in the channel [7], provides an indication of the maximum longitudinal electric field which is the highest for the "C" test ( $I_G/I_D = 3.8 \cdot 10^{-4}$ ), lower for the "B" test ( $I_G/I_D = 3.4 \cdot 10^{-4}$ ) and the lowest for the "A" test ( $I_G/I_D = 1.3 \cdot 10^{-5}$ ).

## EXPERIMENTAL RESULTS

Figure 2 shows the output  $I_D$  and  $I_G$  curves as a function of  $V_{DS}$  of a device before (continuous line) and after (dashed lines) the "B" stress ( $V_{DS} = 5.5$  V and  $V_{GS} = 0$  V for 1000 hrs). An increase in  $I_D$  after accelerated testing is clearly visible. Moreover, the on-state breakdown voltage increases, as it is testified by the decrease in output conductance which can be noticed at  $V_{DS} > 4.5$  V in open channel conditions.

The gate current  $I_G$  due to impact-ionization decreases after accelerated tests, see Fig. 3. This behavior is correlated with the presence of traps in the devices, which can be studied by means of measurements of the frequency dispersion of transconductance,  $g_m(f)$  [8].

The devices present originally both an down-ward and up-ward transconductance frequency dispersion,  $g_m(f)$ , see Fig. 4. Traps in the access region are responsible for  $g_m(f)$  decreasing on increasing frequency [9,10], with  $E_a=0.4$  eV; DX centers in the AlGaAs donor layer under the gate induce  $g_m(f)$  increase at increasing  $f$  [7]. After accelerated tests, the down-ward peak of  $g_m(f)$  increases its amplitude, see Fig. 5, indicating deep level generation in the gate-drain region by hot carriers.

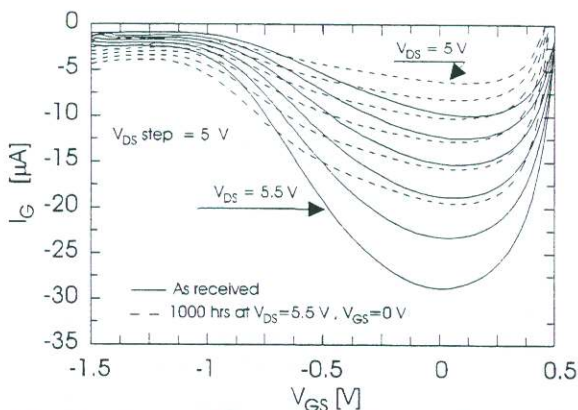


**Fig. 3.**  $I_G$  vs  $V_{GS}$  at different  $V_{DS}$  before (continuous lines) and after (dashed lines) "B" stress test. Decrease of impact ionization is well visible

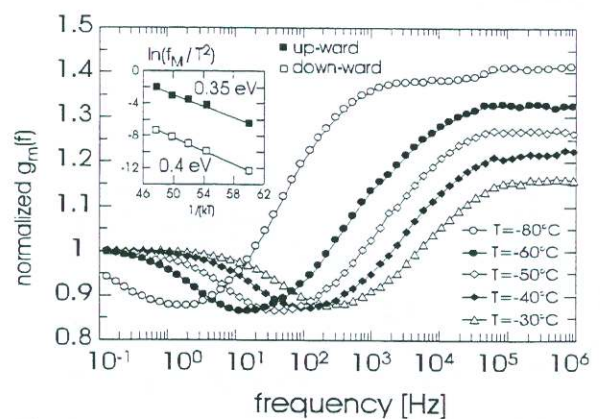


**Fig. 4.** Normalized  $g_m(f)$  measured before stress (bias point:  $V_{DS}=100$  mV,  $V_{GS}=+0.4$  V). Two deep levels ( $E_a=0.35$  eV and  $E_a=0.4$  eV) have been identified.

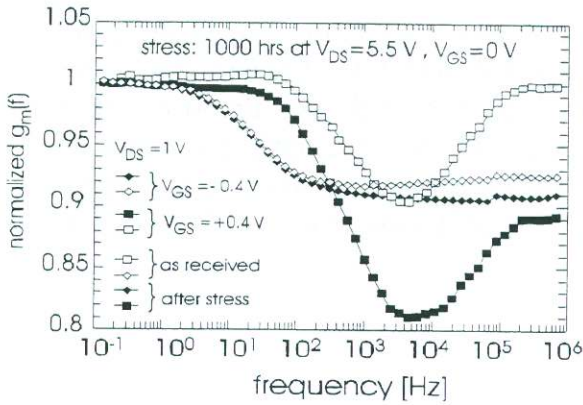


**Fig. 5.** Normalized  $g_m(f)$  before (continuous lines) and after (dashed lines) “B” stress test. Increase in the down-ward  $g_m(f)$  dispersion is observed in open channel condition ( $V_{GS}=+0.4$  V) after stress.

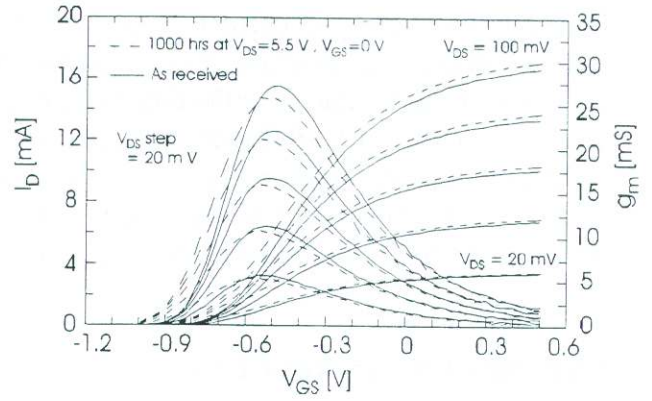


**Fig. 6.**  $I_D$  and  $g_m$  vs  $V_{GS}$  at different  $V_{DS}$  before (continuous lines) and after (dashed lines) “B” stress test. Decrease of threshold voltage is observed after stress.

Figure 6 in fact shows the transconductance,  $g_m$ , measured in linear region, before (continuous lines) and after (dashed lines) “B” stress test. A threshold voltage,  $V_T$ , shift without any significant changing in the  $g_m$  amplitude is observed. This suggest that the increase of  $I_D$  (see Fig.2) is due to a shift of  $V_T$  towards negative values and can not be attributed to any change in the device’s parasitic resistances. The shift of  $V_T$  is also accompanied by a change in the slope of sub-threshold characteristics, as shown in Fig. 7, which confirm the increase in the deep trap density. The reason for threshold voltage decrease is a corresponding decrease in the Schottky barrier height of the gate contact,  $\Delta\Phi_B$ , see Fig. 8. The  $\Delta\Phi_B$  is proportional to the square root of the accelerated test time as occurs in a diffusion-limited process, Fig. 9, and is thermally activated with  $E_a = 0.4$  eV. Decrease of Schottky barrier height after thermal treatments has already been observed for Al/Ti Schottky contacts [11].

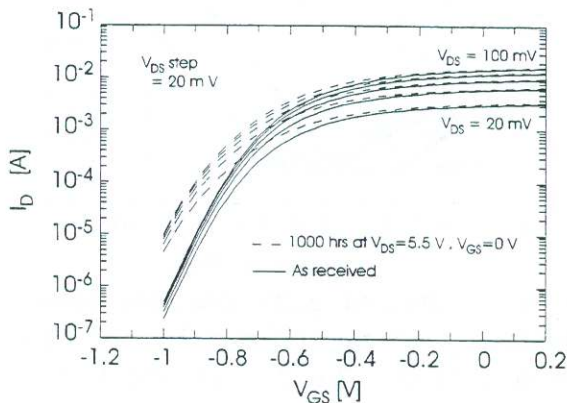


**Fig. 7.**  $I_D$  vs  $V_{GS}$  at different  $V_{DS}$  in semi-logarithmic scale before and after accelerated tests.

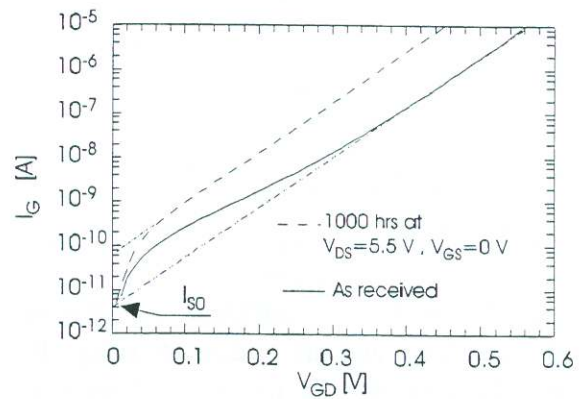


**Fig. 8.** Gate to drain diode forward current before (continuous lines) and after (dashed lines) “B” stress test.



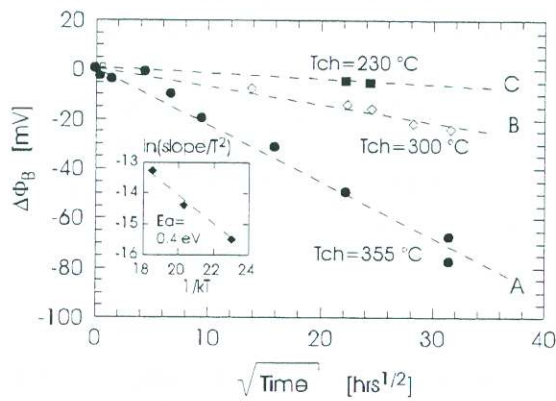


**Fig.9.**  $\Delta\Phi_B$  vs square root of the stress time and of the channel temperature of the device during stress.

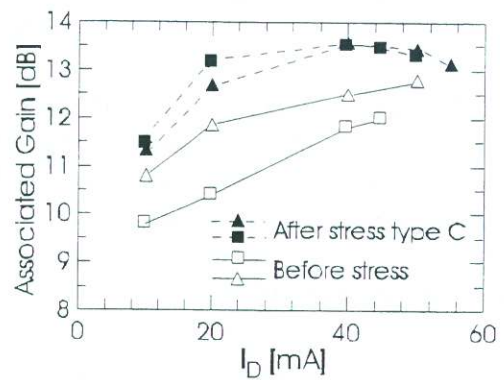


**Fig.10.** Associated gain (measured at 12 GHz) at different current levels  $I_D$ , before and after stress.

Figure 10 shows the associated gain measured at  $f=12$  GHz as a function of  $I_D$ . A non-negligible increase after tests is observed, indicating a possible decrease of the small signal gate capacitance. We also measured all other relevant rf parameters, without identifying significant changes after the tests. In fact, accelerated testing seems to reduce the dispersion and improve slightly the rf performance of these devices.

## DISCUSSION AND CONCLUSIONS

The degradation phenomena in pseudomorphic AlGaAs/InGaAs HEMTs submitted to hot-electron accelerated tests at high power dissipation  $P_D$  have been studied. As received devices present both kink in the output  $I_D$  curves and transconductance frequency dispersion. The downward dispersion of the  $g_m(f)$  has been attributed to traps having an activation energy  $E_a=0.4$  eV and located in the gate-drain and gate-source access regions [9,10]. These traps together with pile-up of holes generated by impact ionization (at the source side) are responsible for the kink phenomena [6]. Other traps, with  $E_a=0.35$  eV, can be located in the AlGaAs donor layer under the gate, may be identified as DX centers have been identified as responsible for the upward  $g_m(f)$  dispersion.

After hot electron and high power dissipation tests, we observe permanent degradation effects, consisting in increasing of  $I_D$ , threshold voltage shift, gate Schottky barrier height decreasing, “breakdown walkout” and increasing in the  $g_m(f)$  dispersion.

The thermally-activated interdiffusion of the Al/Ti gate with decrease in the gate Schottky barrier height is responsible for the  $V_T$  shift and  $I_D$  increase. This mechanism is accelerated by the device self heating.

Traps creation due to hot electrons in the gate-drain access region, with consequent decrease in the longitudinal electric field are responsible for the “breakdown walkout” and for the  $g_m(f)$  increase. Trapping of electrons on these levels induces a decrease in the longitudinal electric field, thus explaining the observed reduction in impact-ionization current and breakdown walkout.



Rather than causing a degradation of the rf characteristics of the device, these phenomena induce an increase in the associated rf gain at 12 GHz, the other rf characteristics being almost unchanged.

In conclusions, we have evaluated failure modes and mechanisms of pseudomorphic HEMTs submitted to tests involving the presence of hot carriers and high power dissipation. Drifts in the DC and low-frequency characteristics have been observed, correlated with generation of deep traps by hot electrons and with thermally-activated gate Schottky barrier height decrease.

## ACKNOWLEDGEMENT

We want to acknowledge Massimo De Feo (University of Padova) for useful discussion and for setting up the low frequency measurements system. This work has been partially funded by the European Space Agency (ESA/ESTEC) under the contract 162367.

## REFERENCES

- [1] C. Canali, P. Cova, E. De Bortoli, F. Fantini, G. Meneghesso, R. Menozzi, E. Zanoni, "Enhancement and degradation of drain current in pseudomorphic AlGaAs/InGaAs HEMT's induced by hot-electrons", Proc. of IRPS 1995, Int. Rel. Phys. Symp. pp. 205-211, 1995.
- [2] G. Meneghesso, C. Canali, P. Cova, E. De Bortoli, E. Zanoni, "Trapped Charge Modulation: A New Cause of Instability in AlGaAs/InGaAs Pseudomorphic HEMT's", IEEE Electron Device Letters, Vol. 17, N.5, pp.232--234, 1996.
- [3] G. Meneghesso, A. Paccagnella, Y. Haddab, C. Canali, E. Zanoni, "Evidence of interface trap creation by hot electrons in AlGaAs/GaAs HEMT's", Applied Physics Letters, Vol. 69, No. 10, pp.1411-1413, 1996.
- [4] R. Menozzi, P. Cova, C. Canali, F. Fantini, "Breakdown walkout in Pseudomorphic HEMT's", IEEE Transaction on Electron DEvices, Vol. 43, No. 4, pp. 543-546, Aprile 1996.
- [5] G. Meneghesso, F. Magistrali, D. Sala, M. Vanzi, C. Canali E. Zanoni, "Failure Mechanisms due to Metallurgical Interaction in Commercially Available AlGaAs/GaAs and AlGaAs/InGaAs HEMT's", Microelectronics and Reliability, Vol. 38, No. 4, pp.497-506, 1998
- [6] T. Suemitsu, T. Enoki, M. Tomizawa, N. Shigekawa, Y. Ishii, "Mechanisms and structural dependence of kink phenomena in InAlAs/InGaAs HEMT's", Proc. of IPRM 97, pp. 365-368, 1997.
- [7] K. Hui, C. Hu, P. George, P. Ko, "Impact Ionization in GaAs MESFET's", IEEE Electron Device Letters, Vol. 11, No. 3, pp. 113-115, 1990.
- [8] C. Canali, F. Magistrali, A. Paccagnella, M. Sangalli, C. Tedesco, E. Zanoni "Trap-related effects in AlGaAs/GaAs HEMTs" IEE Proceedings - Part G, Vol. 138, No.1 p. 104-108, 1991.
- [9] P. H. Ladbrooke, S. R. Blight, "Low-Field Low Frequency Dispersion of Transconductance in GaAs MESFET's with Implication for Other Rate-Dependent Anomalies", IEEE Transaction on Electron Devices, Vol. 35, No. 3. Pp. 257-267, 1988.
- [10] G. Meneghesso, A. Paccagnella, Y. Haddab, C. Canali, E. Zanoni, "Evidence of interface trap creation by hot electrons in AlGaAs/GaAs HEMT's", Applied Physics Letters, Vol. 69, No. 10, pp.1411-1413, 1996.
- [11] Y. Wada, K. I. Chino, "Schottky barrier height variation with metallurgical reaction in aluminum-titanium-galium arsenide contacts", Solid-State Electronics, Vol. 26, pp. 559-564, 1983.